Turbulent Mixing in Baffled Stirred Tanks with Vertical-Blade Impellers

Mixing time and power consumption have been measured in baffled, paddle-agitated cylindrical tanks with single- and double-impellers, and mixing efficiency has been defined by a reciprocal of the product of the mixing time and power consumption. The mixing efficiency and mixing time of double-impeller agitation have been compared with those of single-impeller agitation, and they have been related, through a circulation time, to the flow patterns obtained from the measurements of mean axial and radial velocities.

Satoru Komori, Yasuhiro Murakami
Department of Chemical Engineering
Kyushu University
Hakozaki, Fukuoka 812, Japan

Introduction

Stirred tanks are widely used in the chemical industry as one of the most common mixers, but they are notorious for the complexity of their fluid mechanics. Among these stirred tanks, double- or multiple-impeller stirred tanks have so complex a flow structure that their mixing mechanisms have scarcely been known. Nevertheless, double- or multiimpeller tanks are quite often used for practical purposes, both to get high volumetric mixing or high heat transfer and to reduce the floor area occupied by the equipment in the manufactory. However, whether or not mixing efficiency is truly high in double- or multiimpeller stirred tanks is uncertain, and it should be investigated through fundamental experiments.

Takeda et al. (1968) investigated experimentally the mixing mechanism by conducting both simple flow visualization and measurements of mixing time and power consumption in baffled stirred tanks with double and triple impellers. They suggested that a multiimpeller stirred tank does not always have high mixing efficiency. However, they could not show a conclusive relation between mixing mechanism and flow patterns, since their flow visualization, based on optical observation, was quite insufficient to obtain the exact flow patterns in a turbulent flow with strong recirculating streams. Magelli et al. (1986) also conducted experiments in baffled, stirred tanks with multiple impellers and measured mixing time and power consumption. They examined the fluid-dynamic behavior in terms of both mixing time and the cascade of ideal stages with backmixing, but they could not present a firm relationship between mixing time and fluid-dynamic behavior, such as recirculating streams. Thus the previous studies in multiimpeller stirred tanks are limited to the few investigations cited above, and the details of the mixing mechanism have not been clarified.

The purpose of this work is to explore experimentally the turbulent mixing mechanism and turbulent flow patterns in a baffled, stirred, water tank with double impellers, and to compare double-impeller agitation with single-impeller agitation. Particular attention was paid to the relationship between mixing efficiency and the flow patterns of recirculating streams, which wholly prevail in a tank. Mixing time and power consumption were measured in both double- and single-impeller tanks, and mixing efficiency defined as a reciprocal of the product of the mixing time and power consumption was computed under each operating condition. Under the operating conditions with high or low mixing efficiency, flow patterns were obtained by measuring axial and radial velocities. How the flow patterns affect the mixing efficiency was investigated in terms of a circulation time defined as the traveling time in which a passive tracer starts from a point in a tank at the initial time $t = 0$ and returns to the same point.

Experimental Method

Figure 1 shows an experimental stirred tank and equipment for measuring torque, concentration, and velocity. The stirred water tank used was made of polymethylemethacrylate (PMMA) and was 0.29 m in dia. and 0.7 m in height. The tank had four vertical baffles of 0.029 m radial width. In order to apply a laser-Doppler velocimeter to velocity measurements, the stirred tank was contained in a cubic PMMA tank of side 0.32 m, which was fed with water at the same temperature as in the stirred tank, 293 K.

The impellers used were of the four-blade paddle type and their position could be arbitrarily changed along a rotating axis. The impeller was 0.145 m in dia. and 0.029 m in axial width; its

Correspondence concerning this paper should be addressed to S. Komori.

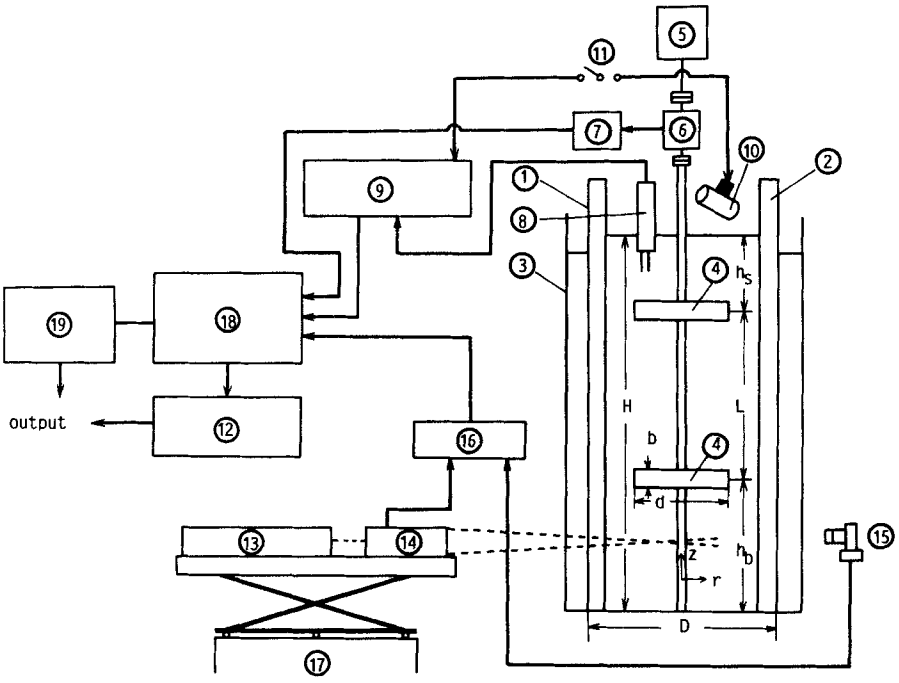

Figure 1. Experimental stirred tank and measuring system.

1. Stirred tank
2. Baffle
3. Cubic tank
4. Impeller
5. D.C. motor
6. Torque transducer
7. Bridge conditioner
8. Conductivity probe
9. Conductivity meter
10. Release device
11. Magnetic switch
12. Pen-recorder
13. Laser
14. LDV optics
15. Photomultiplier
16. Frequency tracker
17. Traversing mechanism
18. Digital data-recorder
19. Digital computer

dimensions and configuration are shown in Figure 2. The phase difference between the blades of double impellers was set to zero. The impellers were driven at speeds of 60, 120, and 150 rpm by a d.c. motor, so that the Reynolds numbers ($Re = nd^2/\nu$) corresponded to 25,000, 48,000, and 62,000, respectively.

Experimental and operating conditions are listed in Table 1. The conditions are divided into five groups, A–E, including single-impeller operations, and they cover almost all conditions that can be considered in single- and double-impeller tanks.

Power consumption was measured by means of a torque transducer connected with a bridge conditioner (Kyowa Dengyo model CDT-307A), and the power due to frictional losses in the bearing was subtracted from the final reading of the bridge conditioner. Accuracy was better than 2% for high values of torque and 5% for low values of torque.

The mixing time θ was measured by examining the concentration fluctuation of a pulse of passive tracer (a KCl solution in this study) as a function of time from its release at $t = 0$. The concentration fluctuation was measured at 0.01 m below the free surface by a conductivity probe connected to a conductivity (concentration) meter. The probe was made from Pt wire of 0.0001 m dia. fitted in a glass tube as described by Benayad et al. (1985) and Rielly and Britter (1985). The frequency response of the probe was roughly estimated to be larger than 50 Hz. The KCl solution was fed from above the free surface by a small release device connected with a magnetic switch; at the same time the concentration meter and a recording system were

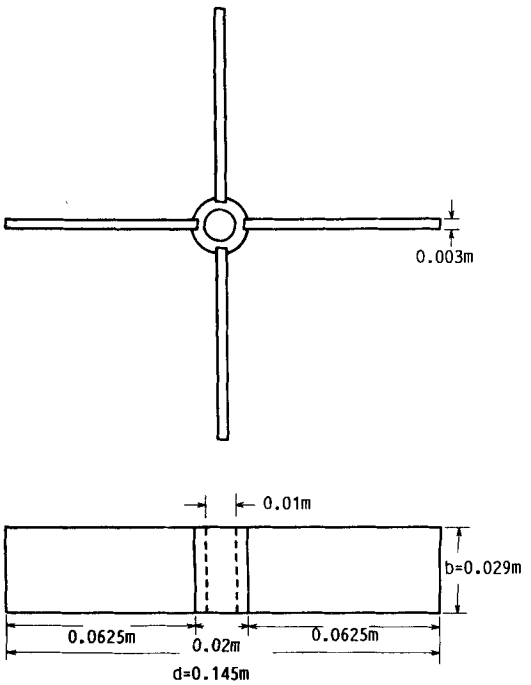

Figure 2. Dimensions and configuration of an impeller.

Table 1. Experimental and Operating Conditions

Group	Water Depth H	No. of Impellers	L/D	h_b/D	n rpm
A	$H = 2D$	2	0.14–1.70	$1.0–0.5L/D$	60, 120, 150
B	$H = 2D$	2	1.0	0.06–0.90	60, 120, 150
C	$H = 2D$	1	—	0.10–1.50	60, 120, 150
D	$H = D$	2	0.10–0.60	$0.5(1.0–0.5L/D)$	60, 120, 150
E	$H = D$	1	—	0.06–0.90	60, 120, 150

operated by the magnetic switch. The mixing time θ was defined as the time from the release of the KCl tracer until concentration fluctuation at the probe was within ±2% of the final reading of concentration.

Instantaneous radial and axial velocities were measured at 150–300 points on the (r, z) plane, Figure 1, by a DANTEC 55X laser-Doppler velocimeter (LDV) with a frequency shifter. The LDV was used in the forward-scatter mode with its optical axes perpendicular to the (r, z) plane, and the Doppler signal was processed with a frequency tracker. The beam spacing was 0.052 m and the focal length of the front lens was 0.25 m. This gave a measuring volume in the form of an ellipsoid of about 0.0003 m dia. and 0.003 m length. The measuring point could be moved on the (r, z) plane by a three-dimensional traversing mechanism. Accuracy of the LDV measurements has been discussed in detail by Komori and Ueda (1985a, b), and the maximum errors by the present measurements were estimated to be within ±0.5% for the mean velocity.

The signals from these instruments were transmitted directly to a digital recorder (TEAC DR-1000) and processed statistically by a digital computer (FACOM M382). The sampling interval was determined to be 0.005 s from both power-spectrum profiles of velocity fluctuations and the sampling theorem in the frequency domain. Sample sizes were 36,000 for the torque, 120,000 for the concentration, and 36,000 for the velocity.

Results and Discussion

Mixing efficiency

It is of great practical importance to obtain high mixing efficiency in stirred tanks. Therefore, the mixing efficiency E was defined by a reciprocal of the product $P \cdot \theta$ of power consumption P and mixing time θ. Mixing efficiency E and energy consumption $P \cdot \theta$ were estimated for all experimental conditions listed in Table 1. Figure 3 shows schematically the quantitative relation between a typical experimental condition and mixing efficiency or energy consumption in each experimental group. It is obvious which of the conditions in each experimental group has high or low mixing efficiency. In order to more clearly compare the mixing efficiency among the experimental groups, an experimental condition with the maximum (highest) mixing-efficiency E_{max}, i.e., the minimum energy-consumptin $P \cdot \theta_{min}$, was sought in each group, A–E, shown in Table 1. Figure 4 shows the values of E_{max} and $P \cdot \theta_{min}$ against given groups. In the cases of groups D and E of a water depth $H = D$, E_{max} and $P \cdot \theta_{min}$ were multiplied by a factor of 0.5 and 2.0, respectively, since the comparison of the mixing efficiency should be done in the same agitation volume as a tank volume with $H = 2D$. It is found that the best operation is single-impeller agitation of group E in a tank of a water depth $H = D$. For a tank of $H = 2D$, the single-impeller agitation of $h_b/D = 1.0$ in group C is also better than the double-impeller agitation. This means that double-impeller

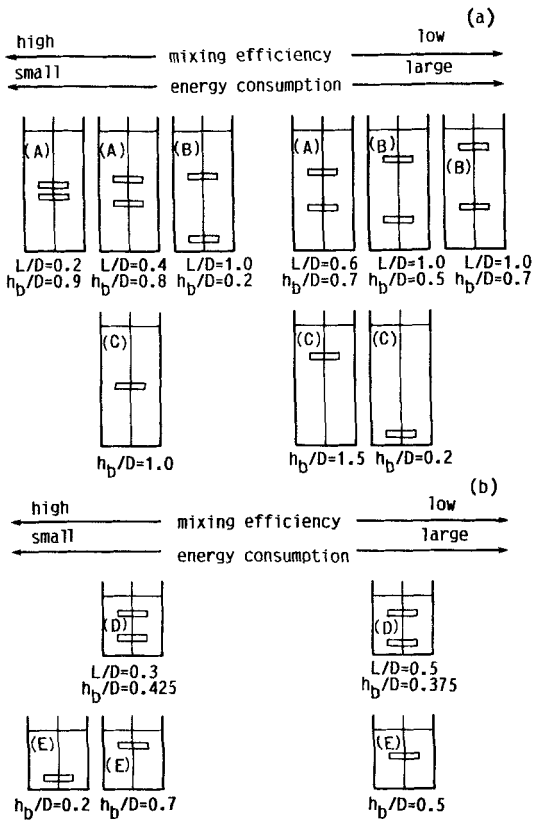

Figure 3. Quantitative relation between typical experimental conditions and mixing efficiency or energy consumption in each experimental group.

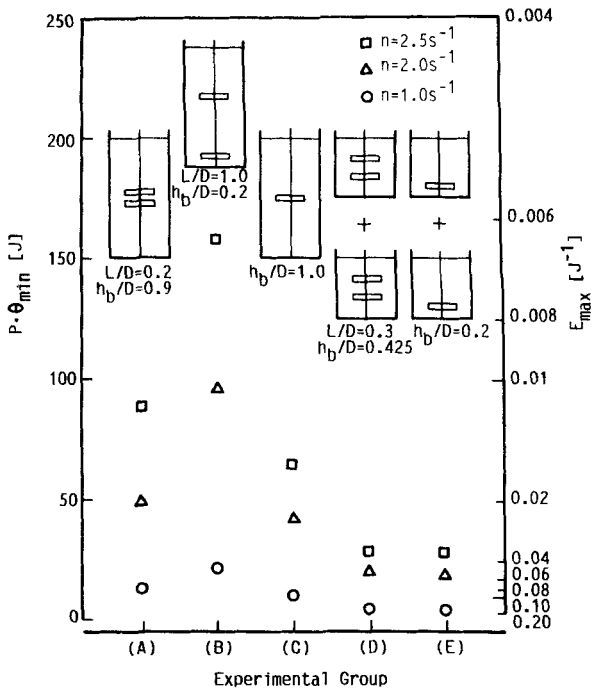

Figure 4. Maximum (highest) mixing efficiency and minimum energy consumption for each experimental group.

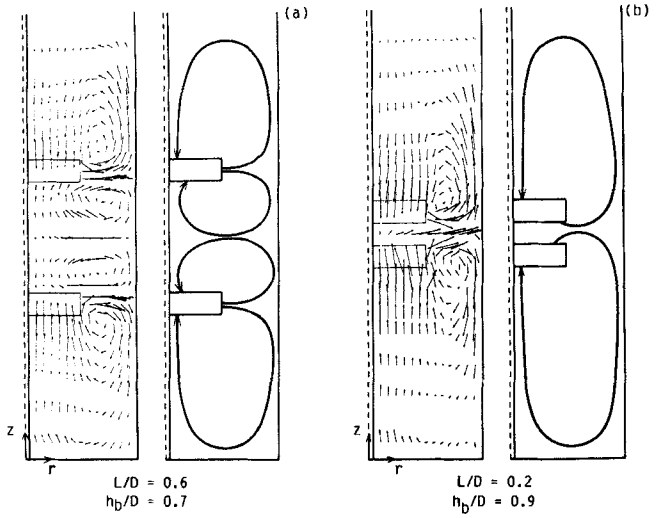

Figure 5. Velocity vectors and flow patterns in a double-impeller tank, $H = 2D$, $n = 150$ (group A).
(a) With lowest mixing efficiency
(b) With highest mixing efficiency

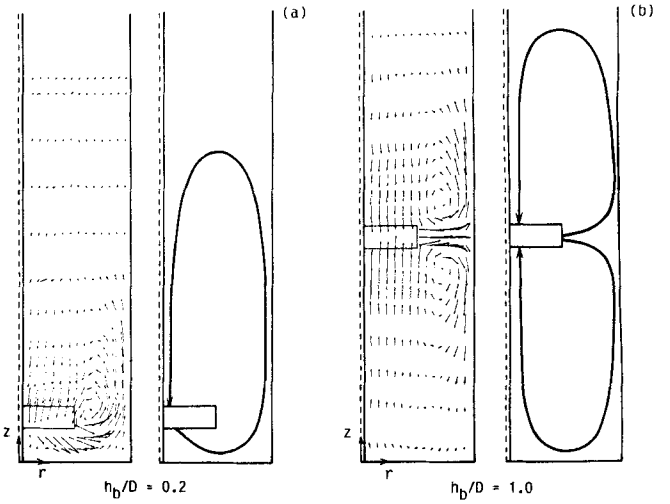

Figure 7. Velocity vectors and flow patterns in a single-impeller tank, $H = D$, $n = 150$ rpm (group C).
(a) With lowest mixing efficiency
(b) With highest mixing efficiency

agitation is ineffective, in particular, for a tank of $H = 2D$. If we were forced to use double-impeller agitation in a tank of $H = 2D$, we would have chosen an agitation condition of $L/D = 0.2$ and $h_b/D = 0.9$ in group A. Further, it is found that E_{max} in group D is slightly smaller than that in group E. This suggests that double-impeller agitation of group D has neither an alternative characteristic nor is of practical interest. The above behaviors of E_{max} and $P \cdot \theta_{min}$ are not affected by impeller rotational speed changes.

Flow patterns

In order to discuss the relationship between flow structure and mixing efficiency, flow patterns were described using the two-dimensional mean velocity vectors measured on the (r, z) plane, Figure 1. These flow patterns are shown in Figures 5–8, together with two-dimensional velocity vectors (V_r, V_z) against both experimental conditions of rotational speed 150 rpm with the highest (maximum) and lowest (minimum) mixing efficiency in each group, except for group D. Here the direction of the velocity vector is denoted by the orientation of the arrows and magnitude by the line length, and the flow patterns are depicted by solid lines which best fit the velocity vectors. When the flow pattern under a condition with the lowest mixing efficiency—(*a*) in Figures 5–8—is compared with that under a condition with the highest mixing efficiency—(*b*) in Figures 5–8—it is found that the number of large-scale recirculating flows

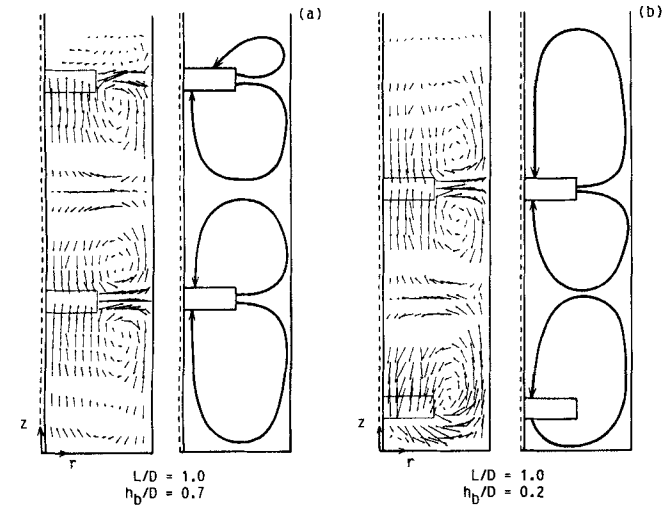

Figure 6. Velocity vectors and flow patterns in a double-impeller tank, $H = 2D$, $n = 150$ rpm (group B).
(a) With lowest mixing efficiency
(b) With highest mixing efficiency

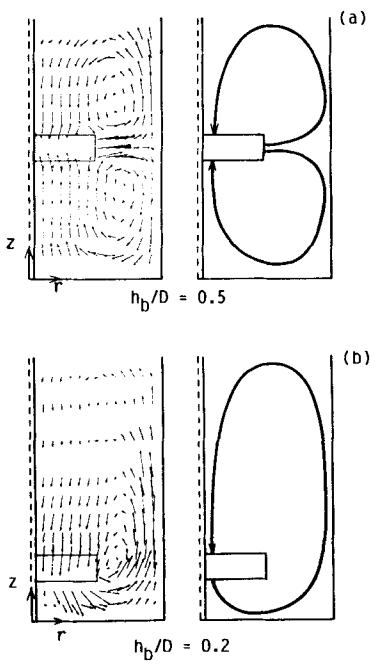

Figure 8. Velocity vectors and flow patterns in a single-impeller tank, $H = D$, $n = 150$ rpm (group E).
(a) With lowest mixing efficiency
(b) With highest mixing efficiency

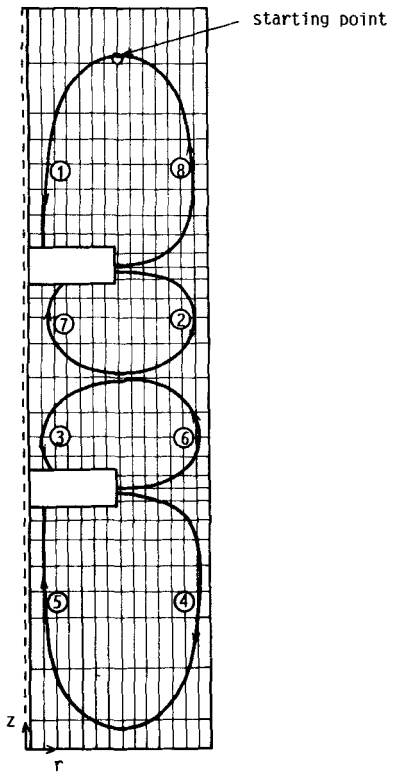

Figure 9. Tracer traveling path and lattices which indicate velocity-measurement points in a double-impeller tank, $H = 2D$, $n = 150$ rpm (group A).

(streams) affects intimately the mixing efficiency and that the smaller number results in higher mixing efficiency. This suggests that the large-scale recirculating flows that prevail in the whole region of a tank are predominant in turbulent mixing in stirred tanks. However, the flow pattern in group C, Figure 7, under a condition with the lowest mixing efficiency is rather special, and the dead space, in which the recirculating flow does not reach, exists in the free surface region. This dead space prevents bulk mixing and disturbs the above relation between the number of recirculating flows and the mixing efficiency.

Relationship between mixing efficiency or mixing time and a circulation time

Effects of large-scale recirculating flows on mixing can be indicated quantitatively by introducing a circulation time T. Circulation time T is defined as the traveling time in which a passive tracer starts from a point near the free surface at an initial time $t = 0$ and returns to the same point. The traveling path of a tracer in the flow shown in Figure 5a is indicated by the successive numbers and solid lines with arrows in Figure 9. Velocity vectors on the traveling path were computed by linearly extrapolating the velocity vectors measured on the lattices shown in the figure, and the traveling time t_i that a tracer takes to travel from a point (r_i, z_i) to a point (r_{i+1}, z_{i+1}) was calculated on each point (r_i, z_i) of the path by

$$t_i = \Delta\ell / |V_i| \qquad (1)$$

where $|V_i|$ is the magnitude of the velocity vector V on a point

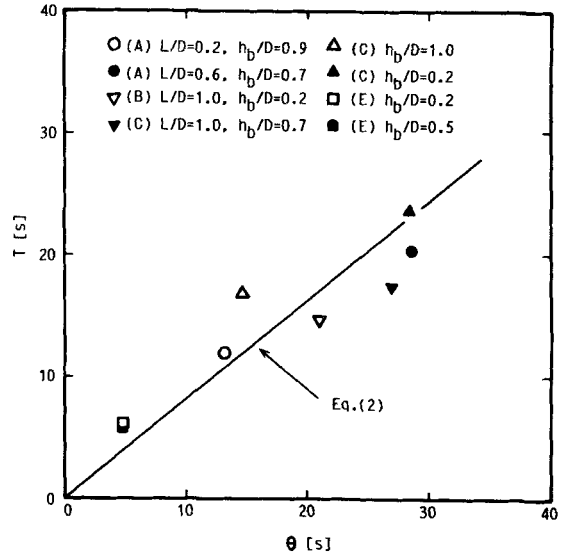

Figure 10. Correlation between circulation time T and mixing time, θ, $n = 150$ rpm.

(r_i, z_i) and $\Delta\ell$ is a small distance along the path between two points (r_i, z_i) and (r_{i+1}, z_{i+1}), which was set to $0.03D$. Finally, the summation of t_i along the traveling path from starting point to final point (i.e., the starting pont) gives circulation time T.

Figure 10 shows the correlation between the circulation time T and the mixing time θ for a rotational speed of 150 rpm. The correlation between T and θ is rather high, and is given by

$$T = 0.83\,\theta \qquad (2)$$

This shows that large-scale recirculating flows, which can be seen from the flow patterns in Figures 5–8, predominate in the mixing in both single- and double-impeller stirred tanks.

To compare the energy consumption $P \cdot \theta$ with circulation time T is physically meaningless, since the dimension of T is quite different from that of $P \cdot \theta$. As mentioned in the previous

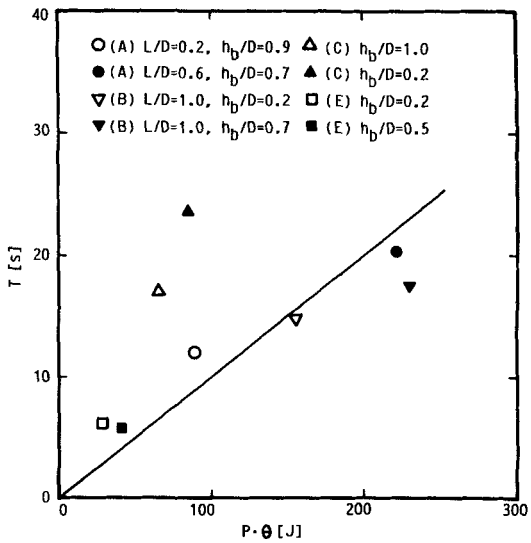

Figure 11. Comparison between circulation time T and energy consumption $P \cdot \theta$, $n = 150$ rpm.

section, however, the energy consumption or mixing efficiency depends strongly on the number of recirculating flows, i.e., on the flow patterns. In this sense, a dependence between T and $P \cdot \theta$ will be expected, because the circulation time T in itself involves the effect of the number of recirculating flows and the flow conditions. Figure 11 shows the comparison between T and $P \cdot \theta$ for a rotating speed of 150 rpm. Except for the data of group C, the strong dependence between T and $P \cdot \theta$ can be seen, as indicated by the straight line. This means that the recirculating flows also dominate mixing efficiency in stirred tanks.

From the facts shown in Figures 10 and 11, one notices that effective mixing can be attained by reducing the circulation time T. To reduce the circulation time, strong larger scale recirculating flows, which prevail in the whole region of a tank, should be created, and the number of recirculating flows in a tank should generally be reduced. This suggests how to design agitation operations.

Conclusions

Turbulent mixing in baffled, stirred tanks with double and single impellers has been investigated experimentally by measuring mixing time, power consumption, and two-dimensional flow patterns on the (r, z) plane. The main results from this study can be summarized as follows.

1. Turbulent mixing in both single- and double-impeller tanks is strongly dominated by large-scale recirculating flows, which prevail in the radial and axial directions. Higher mixing efficiency can be attained by creating larger scale recirculating flows and by reducing the number of the recirculating flows in a tank. A double-impeller tank has more recirculating flows than a single-impeller tank, and in the sense of mixing efficiency double-impeller agitation is inferior to single-impeller agitation.

2. A circulation time, defined as the traveling time of a tracer on the flow patterns, is a useful parameter in estimating the magnitudes of mixing time and energy consumption (or mixing efficiency). A smaller circulation time can generate more effective mixing in both single- and double-impeller tanks.

Acknowledgment

The authors express their appreciation for help given by M. Tanaka, H. Ohtani, and F. Anzai, and they thank H. Ueda for extensive discussions. Partial financial support provided by the Nissan Science Foundation is gratefully acknowledged.

Notation

b = impeller width
D = tank diameter
d = impeller diameter
E = mixing efficiency
E_{max} = maximum (highest) value of E
H = water depth
H_b = vertical distance between bottom of a tank and center of a lower impeller
h_s = vertical distance between free surface and center of an upper impeller
L = vertical distance between double impellers
n = impeller rotational speed
P = power consumption
$P \cdot \theta$ = energy consumption
$P \cdot \theta_{min}$ = minimum value of $P \cdot \theta$
Re = Reynolds number, $Re = nd^2/\nu$
r = radial coordinate
r_i = radial coordinate on a lattice of a traveling path
T = circulation time
t_i = traveling time a tracer takes to travel between two points (r_i, z_i) and (r_{i+1}, z_{i+1})
$|V_i|$ = magnitude of mean velocity vector $V = (V_r, V_z)$ on a point (r_i, z_i)
V_r = mean velocity in radial direction
V_z = mean velocity in axial direction
z = axial coordinate
z_i = axial coordinate on a lattice of a traveling path

Greek letters

$\Delta\ell$ = small distance along a traveling path between two points (r_i, z_i) and (r_{i+1}, z_{i+1}), $\Delta\ell = 0.03D$
θ = mixing time
ν = kinematic viscosity

Literature Cited

Benayad, S., R. David, and G. Cognet, "Measurement of Coupled Velocity and Concentration Fluctuations in the Discharge Flow of a Rushton Turbine in a Stirred Tank," *Chem. Eng. Process.*, **19,** 157 (1985).

Komori, S., and H. Ueda, "The Large-Scale Structure in the Intermittent Region of the Self-Preserving Round Free Jet," *J. Fluid Mech.*, **152,** 337 (1985a).

———, "Turbulent Flow Structure in the Near Field of a Swirling Round Free Jet," *Phys. Fluids,* **28,** 2075 (1985b).

Magelli, F., D. Fajner, G. Pasquali, and M. Nocentini, "Fluid-Dynamic Behavior and Mixing Times of Multiple-Impeller Stirred Tanks with Low-Viscosity Liquids," *Proc. 5th Yugoslav-Austrian-Italian Chem. Eng. Conf.,* Portoroz, Yugoslavia (1986).

Rielly, C. D., and R. E. Britter, "Mixing Times for Passive Tracers in Stirred Tanks," *Proc. 5th Eur. Conf. Mixing,* 365 (1985).

Takeda, K., T. Hoshino, H. Taguchi, and T. Fujii, "Characteristics of the Mutliple Impeller in Turbulent-Mixing Operation of a Deep Vessel," (in Japanese), *Kagaku Kogaku,* **32,** 376 (1986).

Manuscript received Sept. 25, 1987, and revision received Dec. 21, 1987.